NANO LETTERS

Letter

pubs.acs.org/NanoLett

Self-Assembled DNA Nanopores That Span Lipid Bilayers

Jonathan R. Burns,[†] Eugen Stulz,[‡] and Stefan Howorka*,[†]

[†]Department of Chemistry, Institute of Structural Molecular Biology, University College London, London WC1H 0AJ, England, United Kingdom

[‡]Department of Chemistry, University of Southampton, Southampton, SO17 1BJ, England, United Kingdom

Supporting Information

ABSTRACT: DNA nanotechnology excels at rationally designing bottom-up structures that can functionally replicate naturally occurring proteins. Here we describe the design and generation of a stable DNA-based nanopore that structurally mimics the amphiphilic nature of protein pores and inserts into bilayers to support a steady transmembrane flow of ions. The pore carries an outer hydrophobic belt comprised of small chemical alkyl groups which mask the negatively charged oligonucleotide backbone. This modification overcomes the otherwise inherent energetic mismatch to the hydrophobic environment of the membrane. By merging the fields of nanopores and DNA nanotechnology, we expect that the small membrane-spanning DNA pore will help open up the design of entirely new molecular devices for a broad range of applications including sensing, electric circuits, catalysis, and research into nanofluidics and controlled transmembrane transport.

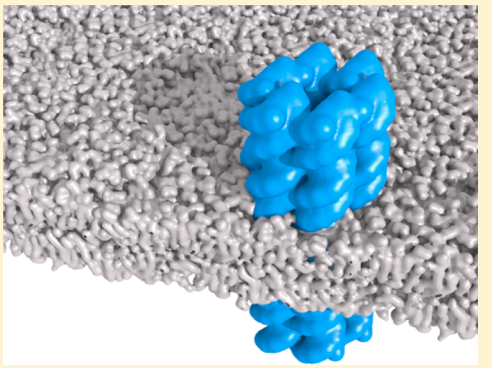

KEYWORDS: *DNA-nanotechnology, nanopore, self-assembly, nucleic acids, origami, single-molecule, lipid bilayer, biophysics, phosphorothioate*

DNA nanotechnology excels at rationally designing bottom-up structures of sophisticated architecture and functionality[1−7] that often mimic naturally occurring proteins. DNA origami can replicate the function of molecular motors,[8−11] antibodies,[12,13] and multienzyme complexes,[14,15] but the large class of bilayer-spanning pores and ion channels is conspicuously missing.

Membrane-spanning nanopores are widespread in nature and facilitate the essential transport of water-soluble molecules across bilayers.[16] Replicating this key property with engineered or de novo pores is scientifically intriguing and additionally leads to powerful biomedical research tools and biosensor elements[17−37] as demonstrated by a variety of rationally designed nanopores composed of protein, peptide, or polymers.[38−40] DNA has also been used to generate synthetic nanofunnels, but these were threaded into hydrophilic solid-state pores.[41] Very recently, a membrane-spanning DNA origami pore has been published.[42,43] It features aromatic membrane anchors and a membrane-piercing nanobarrel with native, negatively charged phosphodiester backbone groups which disrupt the local lipid bilayer structure. Another strategy for membrane insertion is to mimic membrane proteins that feature an outer hydrophobic surface. Following this route, the aim toward membrane-inserting DNA nanobarrels is to overcome the unfavorable energetic interaction between the hydrophobic environment of the membrane and the hydrophilic, negatively charged phosphate groups in the outer pore wall.

Here we enlist targeted chemical modification of nucleic acids[44−47] to generate a DNA nanopore that carries a charge-neutral and hydrophobic, externally facing belt to overcome the energetic barrier toward bilayer insertion. The chemically modified pores are structurally stable and support the transmembrane flow of water as established with a range of analytical techniques. We expect that the simple design of our membrane-spanning DNA pores will help to open up the design of entirely new molecular devices for a broad range of applications including sensing, electric circuits, catalysis, and research into nanofluidics and controlled transmembrane transport.

Results and Discussion. The structure of the DNA nanopore is schematically illustrated in Figure 1. A hollow DNA barrel with an outer width of 5.5 nm and a height of approximately 15 nm is formed by six duplexes that enclose a 2 nm wide central channel (Figure 1A, Supporting Information Figure S-1). The nanobarrel architecture thus follows the principle structural layout of hexagonal arrayed DNA duplexes.[48,49] Reflecting the pore's rational design using scaffold and staple-strands,[3,50] the duplexes are connected either via two antiparallel cross overs in the middle of the origami or an internal antiparallel crossover and two single crossovers at the terminal ends (Figure 1B). The unique and defining characteristic of the barrel is the 2.2 nm long outer hydrophobic ring (Figure 1A, magenta) which matches the thickness of the lipid bilayer[51] (Supporting Information Figure S-2). Unlike conven-

Received: November 9, 2012
Revised: April 21, 2013

   dx.doi.org/10.1021/nl304147f | Nano Lett. XXXX, XXX, XXX−XXX

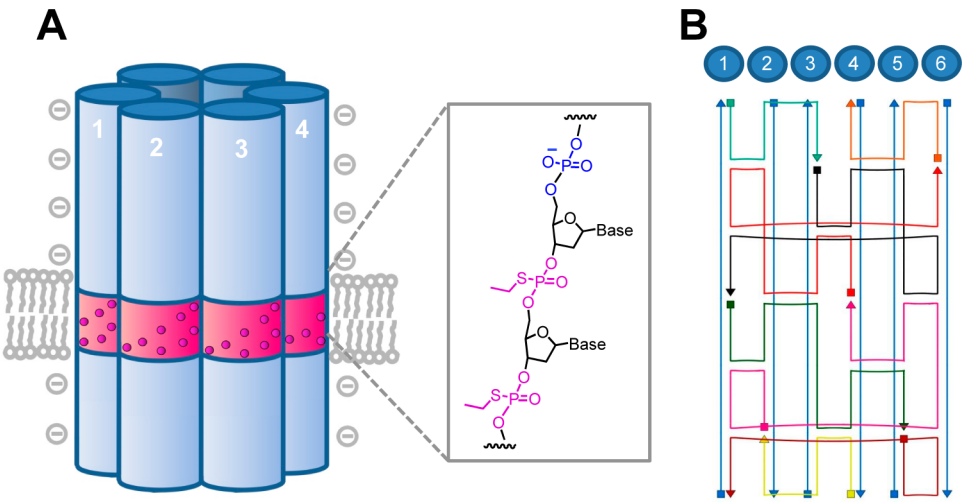

Figure 1. Schematic representation of a DNA nanopore composed of six interconnected duplexes represented as cylinders. (A) On the external face, the barrel features a membrane-spanning hydrophobic belt (magenta) where conventional phosphates of the DNA backbone are substituted by charge-neutral phosphorothioate-ethyl groups (inset). For reasons of clarity, only one stereoisomer of the ethane-PPT group is drawn. (B) Map of the DNA nanostructure with six duplexes (numbered) being formed by six vertical scaffold strands (blue) and eight colored staple strands which run horizontally in conventional honeycomb fashion.

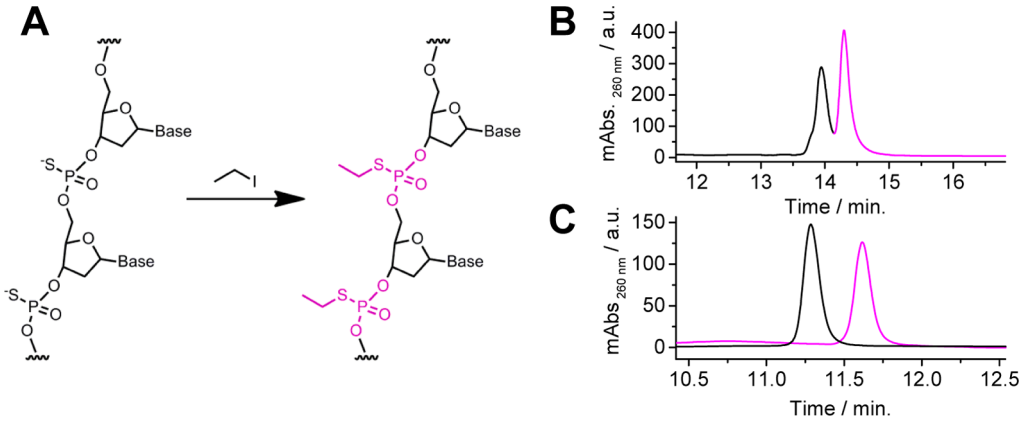

Figure 2. Generation of ethyl-phosphorothioate DNA. (A) Reaction scheme for the modification of PPT-DNA with iodo-ethane. (B, C) HPLC traces determine the extent of modification for a DNA strand carrying a single phosphorothioate group under reaction conditions (B) 10 equiv of iodo-ethane, 55 °C, 1.5 h, and (C) 20 equiv of iodo-ethane, 65 °C, 1.5 h. Panel B shows the trace of the product mixture with unreacted (black) and ethyl-modified phosphorothioate DNA (purple), while C displays the traces of starting material (black) and product mixture (purple). The elution times of the peaks in B and C differ due to the use of two different elution gradients. The extent of modification was confirmed in two additional independent experiments (not shown).

tional DNA, the hydrophobic belt features charge-masked alkyl-phosphorothioates (PPT) with an ethyl moiety attached to the thiol group (Figure 1A, inset), thereby annulling the typical negative charge of a phosphate anion. A total of 72 PPT groups (12 per each duplex) makes up the hydrophobic belt.

The synthesis of the DNA barrel started with the chemical modification of commercially available PPT-containing DNA oligonucleotides to generate charge-capped ethyl-PPT moieties (for sequences see Supporting Information, Table S-1). The DNA strands were subjected to a modification protocol in which ethyl iodide reacts with the thiol group via nucleophilic substitution to yield the ethyl-protected PPT (Figure 2A).[52] The chemical modification achieved a yield of 70% or 100% as determined by high-performance liquic chromatography (HPLC; Figure 2B and C), depending on the reaction conditions (see legend to Figure 2). The more challenging complete modification was also attained for DNA barrel strands with 5 and 18 PPT groups (Supporting Information, Figure S-4). Furthermore, the chemical change of the ethyl modification was successfully confirmed by mass spectrometry (Supporting Information, Figure S-5). We note that, in the subsequent experiments, barrels formed from 70% or 100% modified PPT-DNA strands had the same biophysical characteristics except that the latter were of 5 °C lower thermal stability as determined by UV-melting profiles (Supporting Information, Figure S-6). In the following, we show data of the 70% barrels.

The barrel was assembled by heating and cooling an equimolar mixture of all component strands which includes six ethyl-PPT modified scaffold strands and eight staple strands (Figure 1B; Supporting Information, Table S-1 and Figure S-3). The purity and size of the assembly product were assessed by size exclusion chromatography (SEC) and found to result in a major chromatographic peak corresponding to a 70% yield of formation (Figure 3, blue line; data for 70% modification). In agreement with a hollow DNA barrel, the peak's apparent MW of 500 kDa—obtained by comparison with molecularly

dx.doi.org/10.1021/nl304147f | Nano Lett. XXXX, XXX, XXX–XXX

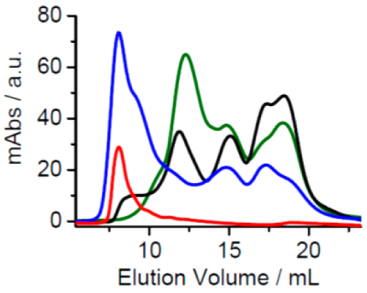

Figure 3. Nanobarrels are formed at high yield and specificity. Size exclusion chromatographic analysis of assembly products from a complete set of DNA strands (blue line), minus two scaffold strands (green), minus four scaffold strands (black line), and the reinjected major peak at 8.15 mL of the completed assembly (red). The assembly mixtures contained 0.5 nmol of DNA each and were run in 1.85 M KCl, 50 mM Tris pH 8.0 at 8 °C.

compact protein standards—is much higher than the origami's actual mass of 156 kDa. The formation of the rationally designed structure was also supported by control experiments where DNA mixtures missing two or four staple strands yielded distinctly smaller complexes (Figure 3, green and black lines).

The chromatographically purified major peak of the complete DNA barrel (Figure 3, red line) was used for the ensuing characterization of the barrel. For example, UV melting profiles established that the assembly process was cooperative as inferred from the presence of a single as opposed to multiple melting transitions (Supporting Information, Figure S-6). Similarly, gel electrophoresis established that the PPT-barrel is stable and migrates as a single sharp band (Supporting Information, Figure S-7), whereas modification with ethyl-iodide decreased the stability, but this is also observed for other DNA nanostructures due to the destabilizing effect of the low-ionic-strength gel electrophoresis buffer.[53]

The monomeric nature and the dimensions of the DNA nanopore were confirmed by dynamic light scattering (DLS)[54] and atomic force microscopy (AFM). A single major DLS peak in combination with the absence of additional higher-order signals (Figure 4A, blue line) implies that only a monomeric species but no aggregates of multiple barrels had formed. The

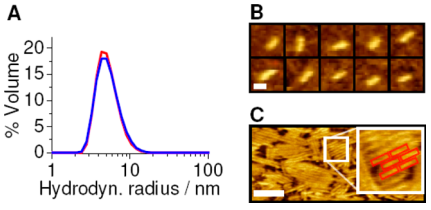

Figure 4. Nanobarrels are monomeric and of the expected dimensions. (A) Dynamic light scattering traces of ethane-PPT-modified DNA origami at pH 8.0 (blue line) and pH 5.0 (red line) featuring a single peak at 4.4 ± 0.1 nm. The average and standard deviation was derived by averaging nine traces acquired using two independently prepared samples. The sample concentration was 0.25 μM. (B) AFM micrograph of individual DNA-nanobarrels adsorbed at a concentration of 5 nM on mica. The images were taken from a larger AFM micrograph (Supporting Information, Figure S-8). (C) AFM micrograph of arrays of tubes with end-to-end-stacked DNA barrels obtained when adsorbing DNA barrels at a concentration of 100 nM onto mica (see also Supporting Information, Figure S-10). The inset shows a magnified view and a schematic drawing of end-to-end arranged DNA nanobarrels. Scale bar, 100 nm.

peak's radius at 4.4 ± 0.1 nm is in good agreement to the calculated value of 4.8 nm;[55,56] the slight difference in size is within the accuracy of DLS measurements for other DNA nanostructures.[56,57] Direct visualization via AFM (Figure 4B,C) confirmed that nanobarrels of the expected dimensions had formed. Isolated nanopores adsorbed on atomically flat mica (Figure 4B; Supporting Information, Figure S-8) had a height of 2.2 ± 0.3 nm as expected for a cantilever-compressed[44,58,59] hollow nanostructure. Furthermore, the apparent length (fwhm) of 21.3 ± 4.0 nm and width of 10.3 ± 1.9 nm (n = 40) was, after tip deconvolution,[60] in excellent agreement with the theoretical dimensions of 15 and 5.5 nm (Supporting Information, Figure S-9). The AFM images (Supporting Information, Figure S-8) and particularly those obtained for A higher DNA barrel concentration of 0.1 μM displayed individual or arrays of elongated tubes which had a width identical to the isolated barrels (Figure 4C; Supporting Information, Figure S-10). These tubes represent chains of end-to-end arranged DNA barrels which are stabilized by blunt-end stacking, as observed for other DNA origami structures.[3] We stress that the weakly connected tubes only form at the energetically stabilizing substrate interfaces. In solution, barrels at comparable or higher concentration are monomeric as shown above by DLS and SEC.

Using single channel current analysis, we probed whether the DNA-nanopores can insert into lipid bilayers and support a stable ionic current. Barrel insertion was achieved by forming a lipid bilayer composed of diphytanoyl-phosphatidylcholine, adding the pore solution to the surrounding electrolyte (1 M KCl, 50 mM Tris, pH 5.0), and applying an alternating voltage. The energetic barrier for channel insertion was also reduced by the hydrophobic belt composed of ethyl-modified PPT groups, as nonmodified PPT barrels did not insert, and by neutralizing with the buffer any residual, negatively charged thiol groups of the phosphorothioate groups (pK_a of 5.3–6)[61] that had not been modified with the ethyl group. The pH of the buffer did not change the structure of the DNA barrel as demonstrated by DLS (Figure 4A, red line). Channel insertion was also achieved at neutral pH for DNA barrels with 100%-modified PPT groups, but the data reported here are for 70% PPT barrels acquired at pH 5.0. After membrane insertion, application of a potential of +100 mV (the side of DNA nanopore addition was grounded) generated a constant flow of ionic current through a single pore (Figure 5A; for two consecutive pore insertions see Supporting Information, Figure S-11). As expected for potential-induced current, the signal was zero at 0 mV (Figure 5B) and negative at −100 mV (Figure 5C). The unitary conductance recorded for several DNA nanopores showed a distribution (Figure 5D) with an average of 395 ± 97 pS at 100 mV (n = 19, excluding the two outlying values in the 80 pA bin) which is within the range observed for nanoscale channels. Calculating the theoretical conductance based on the known pore geometry[16] yielded a higher value of 1320 pS, but this is misleading as the theory's basic assumption, that is, the constant mobility of electrolyte ions, is no longer valid for ionic transport in a confined space of our and other nanoscale pores with high aspect ratios.[62] As shown in Figure 5D, the conductance histogram shows some variation from the maximum, implying slightly different pore conformations. However, gating was rarely observed which is usually an indicator of switching between structural states in membrane channels. It is also noted that channels did not pop out of the bilayer membrane under moderate voltages, while higher

dx.doi.org/10.1021/nl304147f | Nano Lett. XXXX, XXX, XXX–XXX

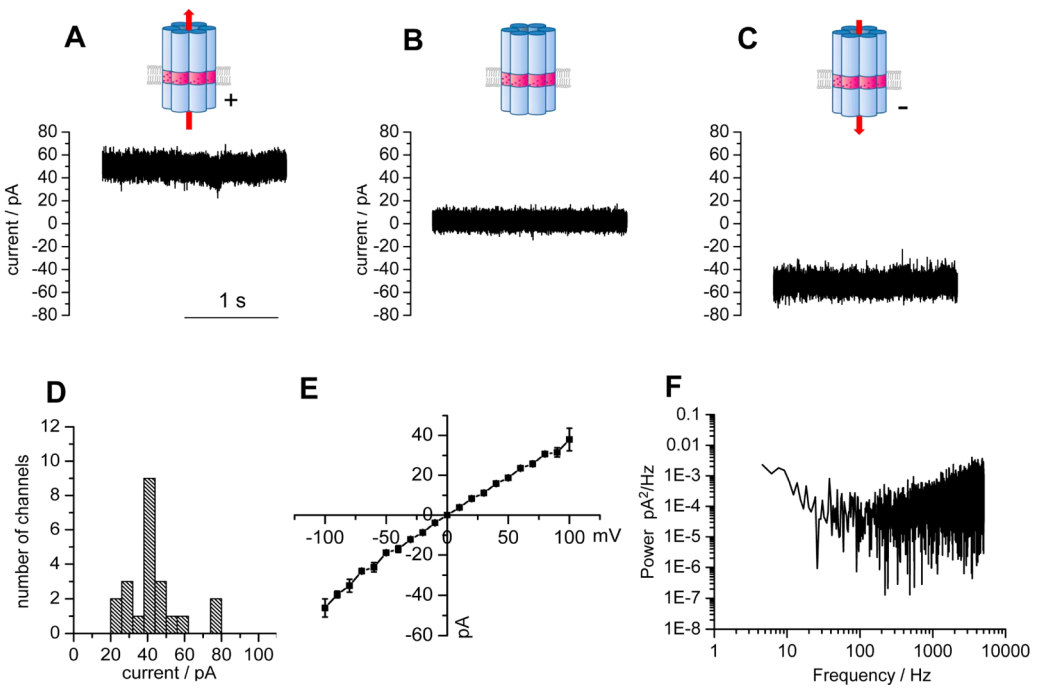

Figure 5. Nanopores are structurally stable in lipid bilayer membranes and support a constant transmembrane current. (A–C) Single channel current trace of a DNA-nanopore in 1 M KCl, 50 mM Tris, pH 5.0 at +100 mV (A), 0 mV (B), and −100 mV (C) relative to the side of the membrane to which the DNA solution was added. The + and − signs indicate the polarity of the potential. The red arrows in the schematic drawings illustrate the flow of K^+ ions through the pore. The traces were filtered at 10 kHz and sampled at 50 kHz. (D) Histogram of pore currents. (E) IV curve of DNA nanopores. The average and standard deviation were derived from five independent recordings from the 40 pA bin from histogram from part D. (F) Power spectrum of the trace in part A.

voltages up to 200 mV caused in several recordings either irreversible channel closure or the expulsion of pore from the membrane (data not shown).

The conductance properties of the DNA nanopores were further investigated to infer information about the structural integrity of the pore. Current recordings are a powerful tool to uncover subtle conformational changes which would be difficult to detect with other single-molecule methods such as AFM or electron microscopy. We first examined the dependence of the nanopores' conductance on the applied potential. The current–voltage curve exhibited a linear, ohmic behavior (Figure 5E) which strongly supports the expected pores' symmetric cylindrical shape.[63] Additional analysis of conductance as a function of recorded signal frequency yielded a power spectrum (Figure 5D). Power spectra can uncover fast conformational changes of subunits or domains in ion channels[64,65] but also alternating ionization states of pore wall residues[66] which is however not applicable in this context due to the low pK_a of the DNA's phosphate groups. The power spectrum (Figure 5F) for the representative DNA nanopore trace of Figure 5A has a very low noise level. The favorable behavior and the absence of a strong $1/f$ noise is comparable to stable protein pores that do not fluctuate. The conductance data support the notion that DNA nanopores maintain their structural stability within the lipid bilayer.

In summary, the generation of a lipid bilayer-spanning DNA origami nanopore is highly relevant in DNA nanotechnology. DNA nanotechnology is in the powerful position to construct a very large variety of nanoscale architectures when compared to the more limited options of other assembly systems composed of peptides or proteins.[67] Despite the tremendous success, up until this report all DNA structures were designed to be soluble in water or to bind onto solid substrate surfaces but not to insert into hydrophobic lipid bilayers.[2] This has deprived the field of the scientifically and biotechnologically important ability to facilitate and control transmembrane transport. With the blueprint for lipid bilayer-spanning DNA origami from this and the recently published paper,[42] DNA nanotechnology can expand into the realm of membrane channels and pores to replicate or transcend the function of biological templates and overcome the limitations of other building materials such as proteins, peptides, and organic polymers which are difficult to assemble into a stable scaffold from scratch. We expect that the new nanopore design will be utilized for next-level DNA nanostructures such as artificial pores with tunable voltage-gating or ion-selective permeation properties, and, possibly, a DNA machine to actively transport matter across a membrane, thereby taking advantage of existing DNA-based molecular motors.[8−11] Building next-generation higher-order nanodevices can utilize our DNA-based membrane pore which is structurally compatible with the honeycomb design of other DNA origami, as illustrated in Supporting Information, Figure S-12.[68]

The new technology for charge-neutralized DNA nanopores combines our research interests in targeted chemical modification of nucleic acids acids[44−47,69] and nanopore engineering.[45,70−73] Importantly, the new technology can also be readily adopted by others. The chemical modification procedure is simple and relies on commercially available DNA oligonucleotides. Optional solid-phase DNA synthesis could also be employed to achieve the generation of charge-masked DNA backbone. As an additional advantage, DNA strands with chemical moieties such as thiol groups are accessible and may assist in the fabrication of, for example. biosensor elements carrying covalently attached ligands for analyte binding.

dx.doi.org/10.1021/nl304147f | Nano Lett. XXXX, XXX, XXX–XXX

In conclusion, our novel design of DNA nanopores synergistically merges the highly productive areas of DNA nanotechnology and nanopores and helps open up exciting research avenues into nanoscale devices for sensing, catalysis, electronics, and research on nanofluidics.

■ ASSOCIATED CONTENT

Supporting Information

Methodological details about the design of the nanopore, alkylation of phosphorothioate-DNA, assembly, and analysis via size exclusion chromatography, UV−vis spectroscopy, dynamic light scattering, atomic force microscopy, gel electrophoresis, and nanopore recordings, as well as additional results on the chemical modification of PPT-DNA with iodo-ethane, melting point analysis of the DNA-nanobarrel, gel electrophoretic migration, AFM analysis, nanopore insertions, and an additional nanopore structure. This material is available free of charge via the Internet at http://pubs.acs.org.

■ AUTHOR INFORMATION

Corresponding Author

*E-mail: s.howorka@ucl.ac.uk. Tel.: 0044 20 7679 4702.

Author Contributions

J.R.B. designed the DNA nanostructures and carried out all experiments except nanopore analysis, E.S. assisted in the selection and optimization of the modification chemistry, and S.H. conducted nanopore recordings, supervised the project, and wrote the manuscript.

Notes

The authors declare no competing financial interest.

■ ACKNOWLEDGMENTS

We thank Julie Herniman at University of Southampton for the mass spectrometric analysis of the DNA oligonucleotides, Dr. Luke Clifton at Rutherford Appleton Laboratories for assisting in performing the DLS measurements, Dr. Richard Thorogate at London Centre for Nanotechnology for the AFM characterization of DNA nanobarrels, Dr. Andreas Ebner and Prof. Peter Hinterdorfer at Johannes Kepler University Linz for discussing AFM analysis, and Astrid Seifert and Nanion for help in acquiring nanopore current recordings. This project was supported by the Leverhulme Trust (RPG-170).

■ REFERENCES

(1) Ding, B.; Seeman, N. C. *Science* **2006**, *314* (5805), 1583−1585.
(2) Lin, C.; Yan, H. *Nat. Nanotechnol.* **2009**, *4* (4), 249−254.
(3) Rothemund, P. W. *Nature* **2006**, *440* (7082), 297−302.
(4) Goodman, R. P.; Schaap, I. A.; Tardin, C. F.; Erben, C. M.; Berry, R. M.; Schmidt, C. F.; Turberfield, A. J. *Science* **2005**, *310* (5754), 1661−5.
(5) Sacca, B.; Niemeyer, C. M. *Angew. Chem., Int. Ed.* **2012**, *51* (1), 58−66.
(6) Teller, C.; Willner, I. *Curr. Opin. Biotechnol.* **2010**, *21* (4), 376−391.
(7) Castro, C. E.; Kilchherr, F.; Kim, D. N.; Shiao, E. L.; Wauer, T.; Wortmann, P.; Bathe, M.; Dietz, H. *Nat. Methods* **2011**, *8* (3), 221−9.
(8) Wickham, S. F.; Bath, J.; Katsuda, Y.; Endo, M.; Hidaka, K.; Sugiyama, H.; Turberfield, A. J. *Nat. Nanotechnol.* **2012**, *7* (3), 169−73.
(9) Omabegho, T.; Sha, R.; Seeman, N. C. *Science* **2009**, *324* (5923), 67−71.
(10) Wickham, S. F.; Endo, M.; Katsuda, Y.; Hidaka, K.; Bath, J.; Sugiyama, H.; Turberfield, A. J. *Nat. Nanotechnol.* **2011**, *6* (3), 166−169.
(11) Venkataraman, S.; Dirks, R. M.; Rothemund, P. W.; Winfree, E.; Pierce, N. A. *Nat. Nanotechnol.* **2007**, *2* (8), 490−4.
(12) Rinker, S.; Ke, Y. G.; Liu, Y.; Chhabra, R.; Yan, H. *Nat. Nanotechnol.* **2008**, *3* (7), 418−422.
(13) Nangreave, J.; Yan, H.; Liu, Y. *J. Am. Chem. Soc.* **2011**, *133* (12), 4490−4497.
(14) Wang, Z. G.; Wilner, O. I.; Willner, I. *Nano Lett.* **2009**, *9* (12), 4098−4102.
(15) Wilner, O. I.; Weizmann, Y.; Gill, R.; Lioubashevski, O.; Freeman, R.; Willner, I. *Nat. Nanotechnol.* **2009**, *4* (4), 249−254.
(16) Hille, B. *Ion channels of excitable membranes*, 3rd ed.; Sinauer Associates: Sunderland, MA, 2001.
(17) Bayley, H.; Cremer, P. S. *Nature* **2001**, *413* (6852), 226−30.
(18) Dekker, C. *Nat. Nanotechnol.* **2007**, *2* (4), 209−215.
(19) Branton, D.; Deamer, D. W.; Marziali, A.; Bayley, H.; Benner, S. A.; Butler, T.; Di Ventra, M.; Garaj, S.; Hibbs, A.; Huang, X. H.; Jovanovich, S. B.; Krstic, P. S.; Lindsay, S.; Ling, X. S. S.; Mastrangelo, C. H.; Meller, A.; Oliver, J. S.; Pershin, Y. V.; Ramsey, J. M.; Riehn, R.; Soni, G. V.; Tabard-Cossa, V.; Wanunu, M.; Wiggin, M.; Schloss, J. A. *Nat. Biotechnol.* **2008**, *26* (10), 1146−1153.
(20) Howorka, S.; Siwy, Z. *Chem. Soc. Rev.* **2009**, *38* (8), 2360−2384.
(21) Cherf, G. M.; Lieberman, K. R.; Rashid, H.; Lam, C. E.; Karplus, K.; Akeson, M. *Nat. Biotechnol.* **2012**, *30* (4), 344−348.
(22) Manrao, E. A.; Derrington, I. M.; Laszlo, A. H.; Langford, K. W.; Hopper, M. K.; Gillgren, N.; Pavlenok, M.; Niederweis, M.; Gundlach, J. H. *Nat. Biotechnol.* **2012**, *30* (4), 349−353.
(23) Clarke, J.; Wu, H. C.; Jayasinghe, L.; Patel, A.; Reid, S.; Bayley, H. *Nat. Nanotechnol.* **2009**, *4* (4), 265−70.
(24) Baker, L. A.; Bird, S. P. *Nat. Nanotechnol.* **2008**, *3* (2), 73−4.
(25) Basore, J. R.; Lavrik, N. V.; Baker, L. A. *Adv. Mater.* **2010**, *22* (25), 2759−63.
(26) Yusko, E. C.; Johnson, J. M.; Majd, S.; Prangkio, P.; Rollings, R. C.; Li, J.; Yang, J.; Mayer, M. *Nat. Nanotechnol.* **2011**, *6* (4), 253−60.
(27) Kasianowicz, J. J.; Brandin, E.; Branton, D.; Deamer, D. W. *Proc. Natl. Acad. Sci. U.S.A.* **1996**, *93* (24), 13770−13773.
(28) Wang, Y.; Zheng, D.; Tan, Q.; Wang, M. X.; Gu, L. Q. *Nat. Nanotechnol.* **2011**, *6* (10), 668−74.
(29) Wanunu, M.; Dadosh, T.; Ray, V.; Jin, J.; McReynolds, L.; Drndic, M. *Nat. Nanotechnol.* **2010**, *5*, 807−814.
(30) Wanunu, M.; Morrison, W.; Rabin, Y.; Grosberg, A. Y.; Meller, A. *Nat. Nanotechnol.* **2010**, *5* (2), 160−5.
(31) Movileanu, L. *Trends Biotechnol.* **2009**, *27* (6), 333−341.
(32) Kowalczyk, S. W.; Kapinos, L.; Blosser, T. R.; Magalhães, T.; van Nies, P.; Lim, R. Y.; Dekker, C. *Nat. Nanotechnol.* **2011**, *6* (7), 433−8.
(33) Venkatesan, B. M.; Bashir, R. *Nat. Nanotechnol.* **2011**, *6* (10), 615−24.
(34) Lu, S.; Li, W. W.; Rotem, D.; Mikhailova, E.; Bayley, H. *Nat. Chem.* **2010**, *2* (11), 921−8.
(35) Powell, M. R.; Cleary, L.; Davenport, M.; Shea, K. J.; Siwy, Z. S. *Nat. Nanotechnol.* **2011**, *6* (12), 798−802.
(36) Albrecht, C. *Nat. Nanotechnol.* **2011**, *6* (4), 195−6.
(37) Wei, R. S.; Gatterdam, V.; Wieneke, R.; Tampe, R.; Rant, U. *Nat. Nanotechnol.* **2012**, *7* (4), 257−263.
(38) Bayley, H.; Jayasinghe, L. *Mol. Membr. Biol.* **2004**, *21* (4), 209−20.
(39) Litvinchuk, S.; Tanaka, H.; Miyatake, T.; Pasini, D.; Tanaka, T.; Bollot, G.; Mareda, J.; Matile, S. *Nat. Mater.* **2007**, *6* (8), 576−580.
(40) Zaccai, N. R.; Chi, B.; Thomson, A. R.; Boyle, A. L.; Bartlett, G. J.; Bruning, M.; Linden, N.; Sessions, R. B.; Booth, P. J.; Brady, R. L.; Woolfson, D. N. *Nat. Chem. Biol.* **2011**, *7* (12), 935−41.
(41) Bell, N. A.; Engst, C. R.; Ablay, M.; Divitini, G.; Ducati, C.; Liedl, T.; Keyser, U. F. *Nano Lett.* **2012**, *12* (1), 512−7.
(42) Langecker, M.; Arnaut, V.; Martin, T. G.; List, J.; Renner, S.; Mayer, M.; Dietz, H.; Simmel, F. C. *Science* **2012**, *338* (6109), 932−936.
(43) The Science paper from ref 42 was published on 16 November 2012 as this Nano Letters paper was under revision.

(44) Mitchell, N.; Schlapak, R.; Kastner, M.; Armitage, D.; Chrzanowski, W.; Riener, J.; Hinterdorfer, P.; Ebner, A.; Howorka, S. *Angew. Chem., Int. Ed.* **2009**, *48* (3), 525−527.
(45) Mitchell, N.; Howorka, S. *Angew. Chem., Int. Ed.* **2008**, *47* (30), 5476−5479.
(46) Mitchell, N.; Ebner, A.; Hinterdorfer, P.; Tampe, R.; Howorka, S. *Small* **2010**, *6* (16), 1732−1735.
(47) Schlapak, R.; Danzberger, J.; Armitage, D.; Morgan, D.; Ebner, A.; Hinterdorfer, P.; Pollheimer, P.; Gruber, H. J.; Schaffler, F.; Howorka, S. *Small* **2012**, *8* (1), 89−97.
(48) Yin, P.; Hariadi, R. F.; Sahu, S.; Choi, H. M.; Park, S. H.; Labean, T. H.; Reif, J. H. *Science* **2008**, *321* (5890), 824−6.
(49) Wang, T.; Schiffels, D.; Cuesta, S. M.; Fygenson, D. K.; Seeman, N. C. *J. Am. Chem. Soc.* **2012**, *134* (3), 1606−16.
(50) Douglas, S. M.; Marblestone, A. H.; Teerapittayanon, S.; Vazquez, A.; Church, G. M.; Shih, W. M. *Nucleic Acids Res.* **2009**, *37* (15), 5001−5006.
(51) Tristram-Nagle, S.; Kim, D. J.; Akhunzada, N.; Kucerka, N.; Mathai, J. C.; Katsaras, J.; Zeidel, M.; Nagle, J. F. *Chem. Phys. Lipids* **2010**, *163* (6), 630−637.
(52) Gut, I. G.; Beck, S. *Nucleic Acids Res.* **1995**, *23* (8), 1367−1373.
(53) O'Neill, P.; Rothemund, P. W. K.; Kumar, A.; Fygenson, D. K. *Nano Lett.* **2006**, *6* (7), 1379−1383.
(54) Clifton, L. A.; Sanders, M. R.; Castelletto, V.; Rogers, S. E.; Heenan, R. K.; Neylon, C.; Frazier, R. A.; Green, R. J. *Phys. Chem. Chem. Phys.* **2011**, *13* (19), 8881−8888.
(55) Ortega, A.; Amoros, D.; de la Torre, J. G. *Biophys. J.* **2011**, *101* (4), 892−898.
(56) Ke, Y. G.; Sharma, J.; Liu, M. H.; Jahn, K.; Liu, Y.; Yan, H. *Nano Lett.* **2009**, *9* (6), 2445−2447.
(57) Kuzuya, A.; Komiyama, M. *Chem. Commun.* **2009**, *28*, 4182−4184.
(58) Leitner, M.; Mitchell, N.; Kastner, M.; Schlapak, R.; Gruber, H. J.; Hinterdorfer, P.; Howorka, S.; Ebner, A. *ACS Nano* **2011**, *5* (9), 7048−54.
(59) Goodman, R. P.; Berry, R. M.; Turberfield, A. J. *Chem. Commun.* **2004**, *12*, 1372−1373.
(60) Klapetek, P.; Ohlídal, I. *Ultramicroscopy* **2003**, *94*, 19−29.
(61) Shibata, A.; Abe, H.; Ito, M.; Kondo, Y.; Shimizu, S.; Aikawa, K.; Ito, Y. *Chem. Commun.* **2009**, *43*, 6586−6588.
(62) Ho, C.; Qiao, R.; Heng, J. B.; Chatterjee, A.; Timp, R. J. *Proc. Natl. Acad. Sci. U.S.A.* **2005**, *102* (30), 10455−10450.
(63) Siwy, Z.; Howorka, S. *Chem. Soc. Rev.* **2010**, *39* (3), 1115−1132.
(64) Starace, D. M.; Bezanilla, F. *Nature* **2004**, *427* (6974), 548−53.
(65) Bezrukov, S. M.; Winterhalter, M. *Phys. Rev. Lett.* **2000**, *85* (1), 202−5.
(66) Bezrukov, S. M.; Kasianowicz, J. J. *Phys. Rev. Lett.* **1993**, *70*, 2352−2355.
(67) Howorka, S. *Curr. Opin. Biotechnol.* **2011**, *22* (4), 485−491.
(68) Song, L.; Hobaugh, M. R.; Shustak, C.; Cheley, S.; Bayley, H.; Gouaux, J. E. *Science* **1996**, *274* (5294), 1859−66.
(69) Borsenberger, V.; Howorka, S. *Nucleic Acids Res.* **2009**, *37* (5), 1477−1485.
(70) Movileanu, L.; Howorka, S.; Braha, O.; Bayley, H. *Nat. Biotechnol.* **2000**, *18* (10), 1091−1095.
(71) Howorka, S.; Cheley, S.; Bayley, H. *Nat. Biotechnol.* **2001**, *19* (7), 636−39.
(72) Howorka, S.; Siwy, Z. S. *Nat. Biotechnol.* **2012**, *30* (6), 506−507.
(73) Borsenberger, V.; Mitchell, N.; Howorka, S. *J. Am. Chem. Soc.* **2009**, *131* (22), 7530−1.